

https://doi.org/10.1070/QEL17997

Phase combining of radiation from a two-channel explosively pumped photodissociation iodine laser with an SBS mirror

S.G. Garanin, Yu.V. Dolgopolov, G.N. Kachalin, A.V. Kopalkin,
S.M. Kulikov, S.N. Pevnyi, F.A. Starikov, S.A. Sukharev

Abstract. **A two-channel double-pass iodine explosively pumped photodissociation laser (EPPL) with an explosively pumped master oscillator (MO) and an SBS mirror is studied. The radiation source, determined by an aperture 6 mm in diameter, through which the radiation from MO enters the turbulent surface air path, is located at a distance of 2.5 km from the amplifier unit input. An SBS mirror with a kinoform raster of microlenses is used to compensate for the amplifier and path optical inhomogeneities and to match the phases in the EPPL channels. The energy and spatial characteristics of the EPPL output radiation are studied experimentally and numerically. Good agreement is obtained between the experimental and calculated distribution of the energy density of the output EPPL radiation in the plane of the MO aperture, which is a pattern of interference between the two channels. The maximum energy density in the aperture plane is by more than 4 times greater than in the case of a single-channel EPPL.**

Keywords: *explosively pumped photodissociation iodine laser, stimulated Brillouin scattering, phase conjugation.*

1. Introduction

The high-power iodine explosively pumped photodissociation laser (EPPL) (λ = 1.315 μm) has a record-breaking pulse energy [1, 2]. The effect of phase conjugation in the process of stimulated Brillouin scattering (SBS) [3, 4] used in a EPPL in the 'master oscillator (MO) + amplifier + SBS mirror' configuration to compensate for optical inhomogeneities of the amplifier and the optical path [5, 6] opens up the possibility of interesting applications in the physics of high energy densities. For example, one of them is the implemented focusing of radiation into a spot of size $\sim\lambda$ [7] with the achievement of energy flux densities and electric field strengths, which otherwise could be achieved only using femtosecond lasers. In this case, it becomes possible to study the interaction of a monochromatic extremal field with matter under virtually quasi-stationary conditions (compared to the characteristic atomic relaxation times).

The progress of EPPL studies is associated with solving two important problems that inevitably appear at a certain stage in the high-power laser development. The first problem is how to increase the radiation energy and radiant intensity. When the potential of the active medium is exhausted, the main hopes become associated with the realisation of a multichannel laser. When phasing radiation in N parallel channels, then, in addition to increasing the power by N times, it is possible to increase the radiant intensity by N^2 times. The second problem relates to the delivery of radiation to the receiver under conditions of an optically inhomogeneous propagation path.

The authors of Refs [5, 6] considered a 'converging' version of the EPPL at a working mixture pressure of 25 Torr C_3F_7J + 125 Torr Xe. To correct the beam quality, use was made of a SBS mirror proposed in [8] with a kinoform raster of diffractive lenses. As a result of optimising the configuration of this SBS mirror by means of a three-dimensional nonstationary SBS computational model [9, 10], the quality of phase conjugation is close to ideal at any laser pump power exceeding the threshold one [10–13]. In a single-channel EPPL, it was possible to achieve the following output radiation parameters: the energy was about 400 J, the radiant intensity was 10^{12} J sr^{-1}, and the Strehl number was at the level of 0.7 (see Figs 1a–1c). Due to the threshold nature of SBS, the EPPL implements a repetitively pulsed regime, in which the repetition period of the output radiation pulses is equal to twice the time it takes for the radiation to travel from the amplifier to the SBS cell. The experimental data are in good agreement with the results of three-dimensional nonstationary simulation of a double-pass EPPL [14], which takes into account diffraction, amplified spontaneous emission of amplifiers, radiation losses in the optical path, inhomogeneous amplification with saturation, and refraction of radiation by optical inhomogeneities of the amplifier active medium caused by the shock wave.

The radiation intensity at the amplifier input, which is provided by a lamp MO, was about 0.2 W cm^{-2} in the experiments. As shown by the calculations, in the presence of parasitic reflections of laser radiation from the optical scheme elements [15–17], if parasitic reflections with a coefficient higher than 10^{-7} are not suppressed, they can significantly reduce the EPPL radiant intensity, which was observed in some experiments (see Figs 1d–1f). According to calculations, to eliminate the effect of parasitic reflections on the EPPL divergence reliably, the MO radiation intensity at the amplifier input should exceed 10–20 W cm^{-2}.

The purpose of this work is to study the operation of the EPPL in a two-channel version with an explosively pumped MO to increase the intensity at the amplifier input. In the two-channel EPPL, the SBS mirror is also of interest because it provides the phase combining of the radiation in a natural way: phasing is a special case of phase conjugation of a fragmentary common beam. Note that phase conjugation at SBS is one of the well-known mechanisms of coherent phase com-

S.G. Garanin, Yu.V. Dolgopolov, G.N. Kachalin, A.V. Kopalkin, S.M. Kulikov, S.N. Pevnyi, F.A. Starikov, S.A. Sukharev Russian Federal Nuclear Centre–All-Russian Research Institute of Experimental Physics (RFNC–VNIIEF), prosp. Mira 37, 607188 Sarov, Nizhny Novgorod region, Russia; e-mail: fstarikov@mail.ru

Received 14 December 2021
Kvantovaya Elektronika **52** (3) 289–295 (2022)
Translated by V.L. Derbov

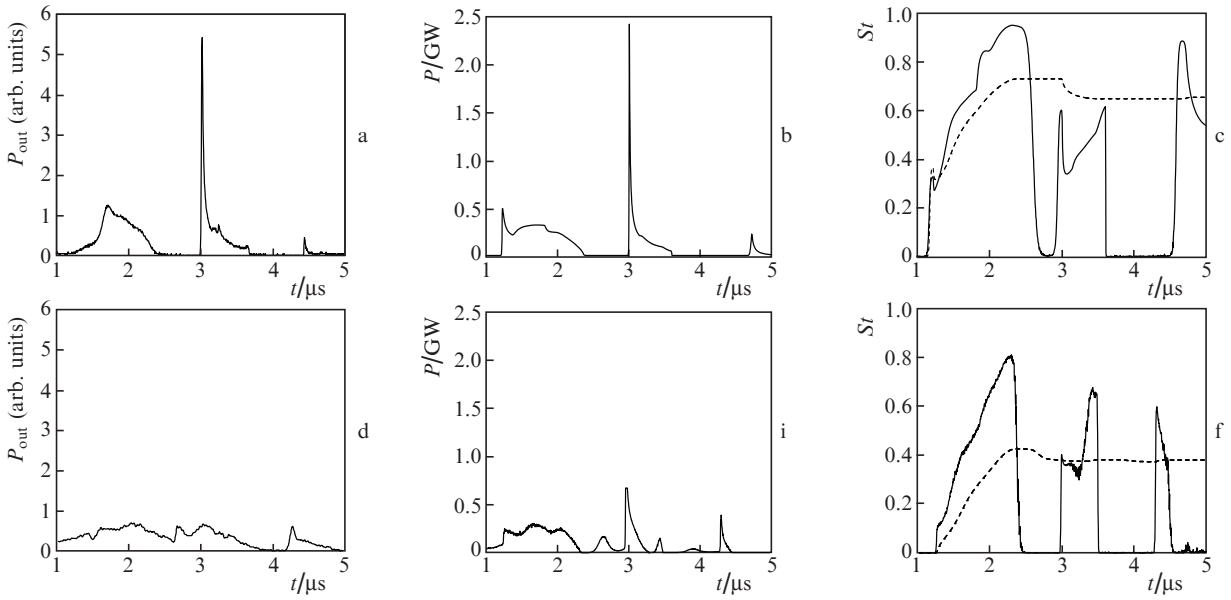

Figure 1. Dynamics of (a, d) experimental and (b, e) calculated power and (c, f) calculated Strehl number of EPPL radiation (a–c) in the absence and (d–f) in the presence of parasitic reflections with a coefficient of 10^{-6}. The dashed line shows the dynamics of the average Strehl number.

bining of multichannel radiation [18–20]. In contrast to the studies, in which a phased wavefront is formed directly at the output of an amplifier unit (see, e.g., [21, 22]), in the present work, a long turbulent atmospheric path is included in the feedback loop. Using three-dimensional nonstationary models [10, 14], a computational study of the two-channel EPPL operation with phase combining of the radiation from two laser channels is carried out using the SBS technique; the calculated results are compared with the experimental ones. The MO radiation source was located in a turbulent atmosphere at a distance of 2.5 km from the amplifier unit input, which is necessary for optical decoupling of the MO from the amplifier unit. The main interest lies in studying the structure of the EPPL radiation beam in the MO region and evaluating the efficiency of phase conjugation under conditions of a turbulent propagation path.

2. Schematic diagram of a two-channel EPPL

The schematic of the EPPL in a two-channel version is shown in Fig. 2. The EPPL contains a master oscillator, two amplifier units with a length $L_{a1} = L_{a2} = 1$ m, located at a distance $L_{12} = 20$ m from each other, and an SBS mirror with an angular selector. The distance L_{23} between the second amplifier and the SBS mirror is 68 m.

In more detail, the optical scheme of the EPPL is shown in Fig. 3, where the MO aperture is number *5*. The two-channel amplifier is implemented in a 'converging' version of the EPPL with a laser mixture 25 Torr C_3F_7I + 125 Torr Xe. To ensure the most compact arrangement of the apertures of the two channels, their amplifying stages [(*11*) and (*12*) in Fig. 3] were shifted along the axes relative to each other by a distance of about 2 m (see Fig. 4).

Two double-stage channels of amplification with 20 m separation between the amplifying stages are arranged parallel to each other with a gap of 31 cm between the optical axes spaced apart in the horizontal plane. The maximally collimated MO radiation is restricted by an aperture located at a distance $L_1 \approx 2.5$ km from the input window of the first pair of amplifiers. As shown by experiments and calculations, in a single-channel 'converging' version of the EPPL with a mixture of 25 Torr C_3F_7J + 125 Torr Xe, the output energy reaches ~400 J, and the radiant intensity is 10^{12} J sr^{-1}. With the full use of the potential of the EPPL active medium, an increase in its energy and brightness is possible only by combining radiation of several channels.

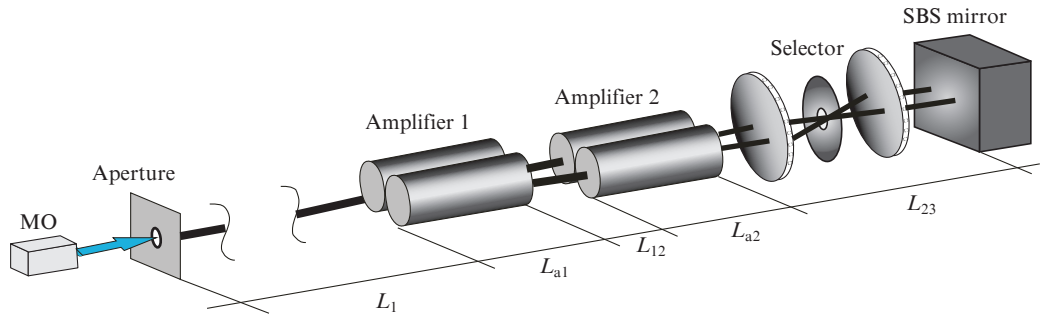

Figure 2. (Colour online) Schematic of a double-pass dual-channel EPPL.

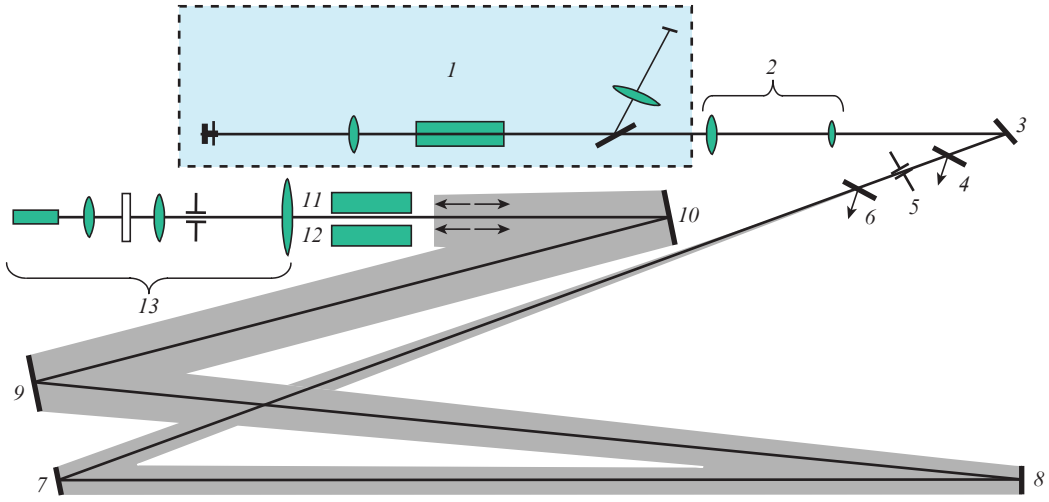

Figure 3. (Colour online) Optical layout of the EPPL with explosively pumped MO: (*1*) explosively pumped MO; (*2*) matching telescope; (*3*, *7–10*) flat mirrors; (*4*, *6*) measuring optical wedges; (*5*) reference (measuring) aperture; (*11*, *12*) EPPL amplifier units; (*13*) SBS mirror with a selector.

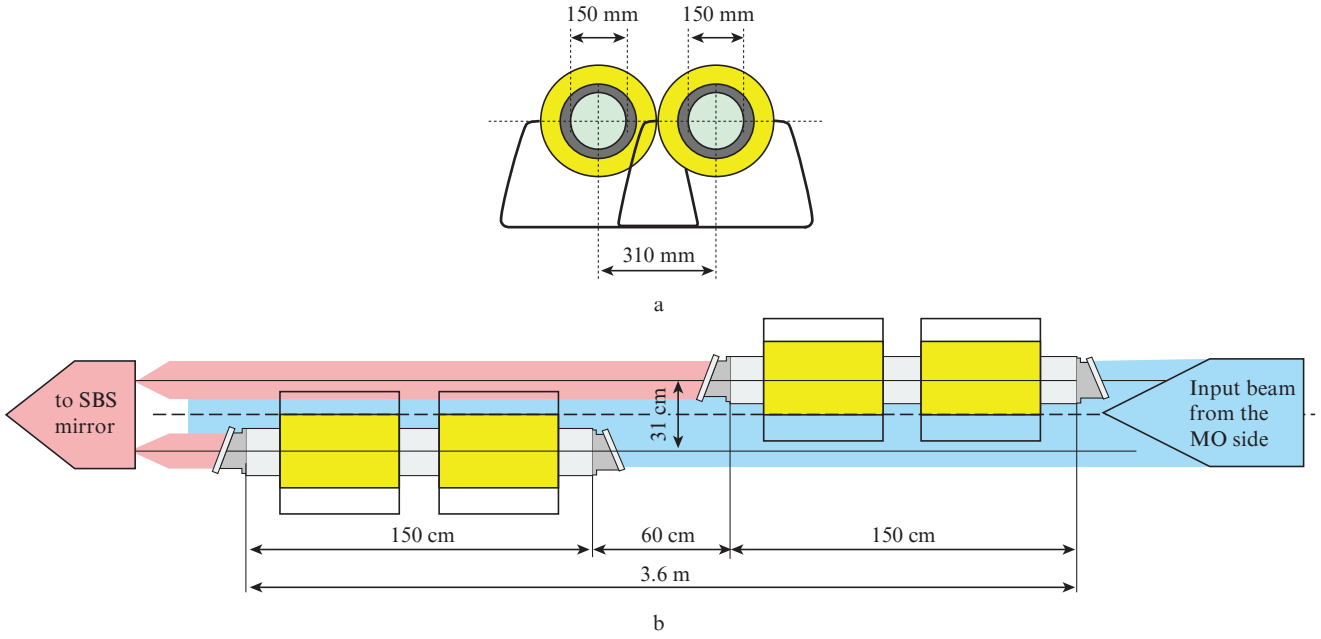

Figure 4. (Colour online) Close packing of apertures of two amplifying channels: (a) view along the axis; (b) top view.

Phase conjugation at SBS was implemented in a high-pressure gas mixture (48.5 atm Xe + 1.5 atm SF_6) [5, 6]. Figure 5 shows the scheme of injecting two parallel beams with an aperture of up to 12 cm, separated by a distance of 31 cm, into the SBS cell. In the scheme, both beams of MO radiation amplified during the first pass (pump radiation) are focused by a lens 650 mm in diameter into a selector of Stokes waves with an angular transmission of 4×10^{-4} rad, and then directed to two identical kinoform rasters of diffractive lenses and focused into an SBS cell.

Thus, the MO radiation passes through the aperture, propagates along a horizontal path 2.5 km long, is amplified in the amplification stage, reaches the SBS mirror and is reflected from it, is amplified in the second pass, and again propagates along a 2.5 km long path. The main goal of this work is to record and analyse the spatial and energy characteristics of the EPPL radiation in the plane of the MO aperture.

3. Master oscillator based on an explosively pumped EPPL

In calculations [15–17], it was found that parasitic reflections from optical scheme elements with a coefficient of 10^{-7}–10^{-6} at the MO signal intensity of 0.2 W cm^{-2} at the amplifier input, which is typical for lamp MO, can significantly increase the divergence of the EPPL output radiation. It was shown that to ensure suppression of parasitic reflections, an input MO signal level of at least 10–20 W cm^{-2} is required; this level can be provided by an explosively pumped MO.

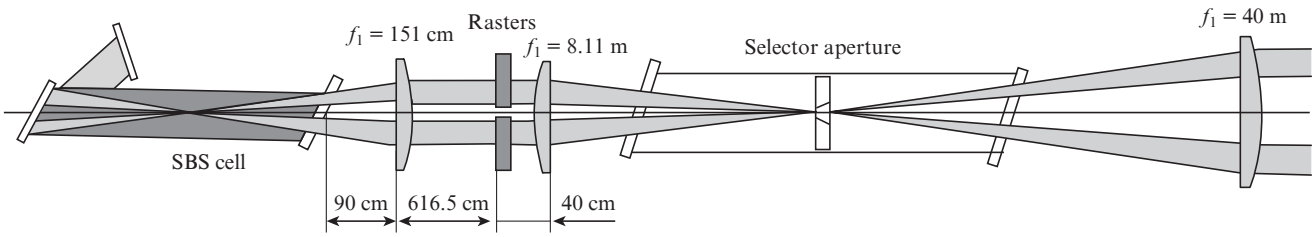

Figure 5. Schematic of the input system for the two-channel EPPL.

To carry out experimental studies on the phase combining of radiation beams from parallel channels of the converging version of the phase-conjugated EPPL, an optical scheme for the formation of MO radiation of diffraction quality at the input of an amplifier unit with an aperture of $D \approx 0.5$ m was developed. The optical scheme (see Fig. 3) has no forming lenses; it is based on the principle of free beam expansion on the atmospheric path after the forming reference aperture. The scheme is equivalent to that of an objective lens with a focal length $F = L_1 \approx 2.5$ km with a reference aperture of diameter d located in its focal plane. For the amplified Stokes radiation, the formation scheme plays the role of a measuring objective lens with a focal length of ~2.5 km. To correctly measure the distribution of the axial intensity of the amplified Stokes radiation in the far-field zone and, therefore, the axial radiant intensity, the diameter of the reference aperture is chosen based on the condition $d = \lambda L_1/D$; as a result, we have $d \approx 0.6$ cm for our scheme.

In the quartz EPPL version, a cylindrical quartz cuvette 1 m long with an inner diameter of 90 mm is filled with a laser mixture and placed in an aluminium cylindrical case 50 cm in diameter and 1 m long (Fig. 6). Ultraviolet pump radiation is emitted by a shock wave propagating in krypton placed in a metal case at a pressure of 1 atm. The source of the shock wave is a cylindrical explosive charge with a diameter of 100 mm and a length of 900 mm. The inner diameter of the quartz tube is $D = 90$ mm. The distance l_k from the explosive charge to the quartz tube was 250 mm.

Let us consider the operation of the master oscillator in a full-scale experiment with amplification and phasing of radiation in parallel EPPL channels with phase conjugation.

A mixture of gases with partial pressures of 5.5 Torr C_3F_7I and 30 Torr SF_6 was used as an active element. Cat's eye reflectors were used for positive feedback in the resonator. The directivity pattern was formed by an aperture 4 mm in diameter placed in front of the rear feedback mirror in the focal plane of a lens with a focal length $f_1 \approx 40$ m. The laser aperture was limited by a diaphragm 40 mm in diameter. Polarised laser radiation with an electric vector oscillation in the vertical plane was ensured in the resonator by the presence of a reflective plate positioned at the Brewster angle to the radiation axis (rotation around the vertical axis). To reduce the optical load on the resonator mirrors, a mirror with a transmission of 50% was placed as a filter (attenuator) in the output leg of the resonator.

The main parameters of MO and its radiation in the experiment are presented below.

EPPL variant	quartz
Quartz tube length/m	1
Inner diameter of the quartz tube/mm	90
Active length/m	0.9
Aperture diaphragm diameter/mm	40
Laser mixture	5 Torr C_3F_7I and 30 Torr SF_6
Angular selector transmission/rad	1×10^{-4}
Effective coefficients	$R_{rear} \approx 0.63$
of resonator mirror reflections	$R_{fr} \approx 0.0035$
Optical length of the resonator/m	160
Output radiation energy/J	12.2 ± 1.8
Average radiation power/W	2.6×10^5
The radiation pulse duration at the 0.1 level of the maximum power/μs	47
Radiation intensity at the amplifier input/W cm^{-2}	
1st channel	4 ± 1
2nd channel	4 ± 1

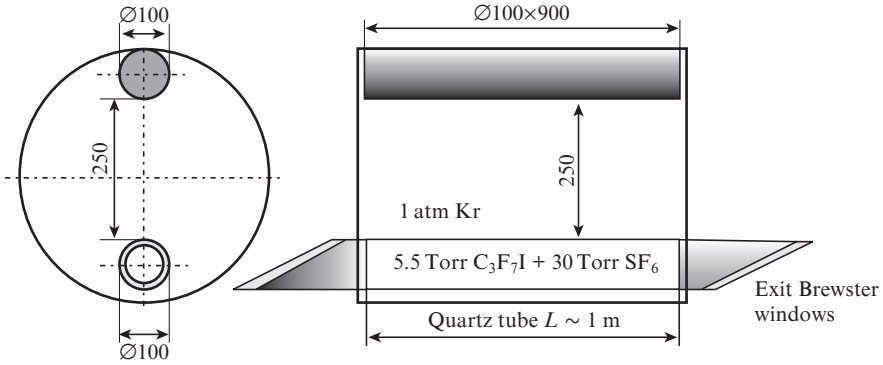

Figure 6. Master oscillator based on a quartz EPPL version (in mm).

The radiation oscillogram at the MO output, obtained in the experiment using G8421-03 InGaAs photodiodes with a time resolution of about 2 ns, is shown in Fig. 7. The spectrum of MO emission exhibits a multimode generation structure in terms of the longitudinal index; 80% of the radiation energy of the MO lies in the spectral range $\Delta f = 68$ MHz, from where the radiation coherence length $l_{coh} \approx c/\Delta f = 4.4$ m. To implement high-quality phase conjugation, it is necessary that the length of the nonlinear interaction region in the SBS cell be less than the coherence length. The quasi-stationary excitation of SBS is also facilitated by the fact that the width of the spectral line of MO radiation is much smaller than the width of the scattering line.

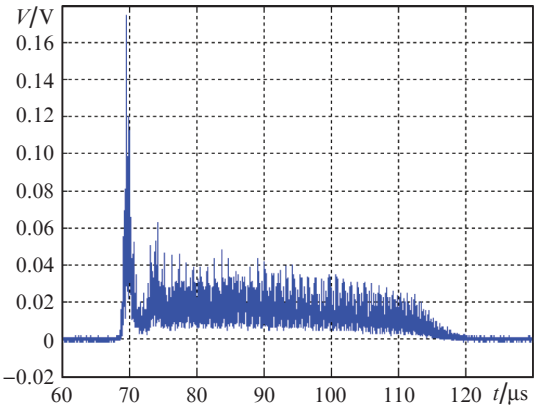

Figure 7. (Colour online) Oscillogram of radiation at the output of the master oscillator.

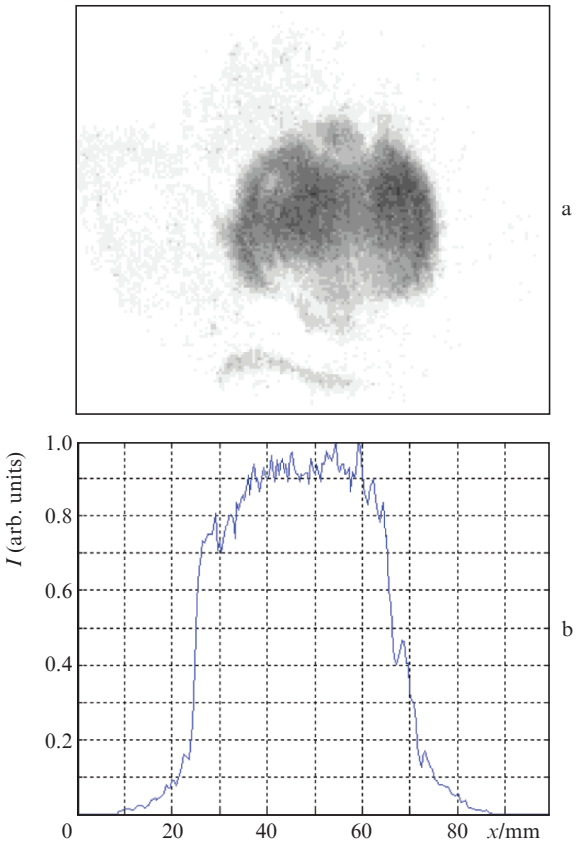

Figure 8. (Colour online) (a) Distribution of the MO radiation energy density and (b) its section along the transverse axis in the near-field zone.

The patterns of MO radiation in the near- and far-field zones are shown in Figs 8 and 9. It was found that, for a radiating aperture diameter 40 mm, the radiation divergence is expected to be about 1×10^{-4} rad.

4. Experimental and calculated results

We performed a computational study of phase conjugation in an SBS mirror with a kinoform lens raster in three-dimensional geometry. Calculations using the model [10] showed that, like in the single-channel version [8–12], in the case of a multichannel input of radiation, there is an optimal geometry of the SBS mirror (see Fig. 5), which provides the quality of wavefront conjugation of more than 90% and a high, stable coefficient of Stokes radiation selection. It is shown that the dephasing (different phase shift) of radiation in the channels does not lead to a deterioration in the quality of phase conjugation. The conjugation quality factor is more sensitive to drops in the intensity of the input radiation in the channels; however, the reduction in the conjugation quality factor to ~85% occurs at drops of 50%–100%. In the experimental layout shown in Fig. 5, the conditions for a high quality phase conjugation were realised: both characteristic zones of increased pump radiation intensity (the focal plane of the lens and the image of the focal plane of the lens raster) were focused into the cell, and rasters with a cell size of 1 mm and a focal length of individual 8-level diffractive lenses 9.5 cm were used.

The EPPL calculation model [14] includes the radiation propagation path, which is an optically inhomogeneous atmosphere. The model for calculating the propagation of

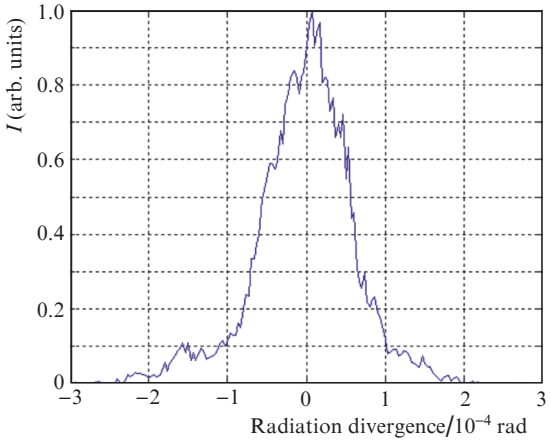

Figure 9. (Colour online) Section of the density pattern of the MO radiation energy in the focal plane of the lens with $F = 60$ m.

radiation in a turbulent atmosphere is described in [23]. A section of the calculated distribution of radiation energy density at the EPPL near-field output on a horizontal moderately turbulent path with a structural constant $C_n^2 = 10^{-15}$ cm$^{-2/3}$ is shown in Fig. 10.

The calculations showed that with a phased input signal from the MO, replacing one EPPL channel with two channels increases the radiant intensity by a factor of 4.4 in the absence of parasitic reflections from optical elements. The output energy increases by a factor of 2.1 (from 430 to 890 J) regard-

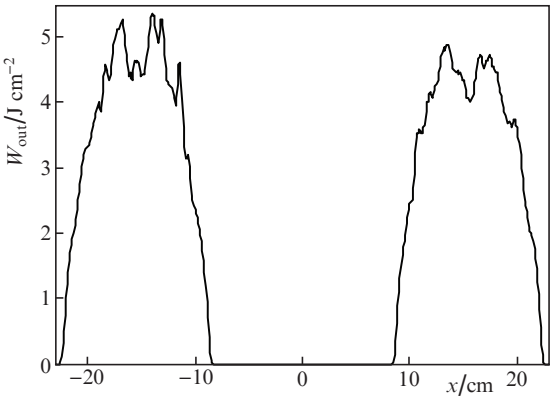

Figure 10. Axial section of the calculated radiation energy density distribution at the EPPL output in the near field at $C_n^2 = 10^{-15}$ cm$^{-2/3}$ in the case of two separated channels with an aperture of 0.6 cm.

less of parasitic reflections. This is explained by the growing SBS mirror reflection coefficient upon a twofold increase in the power of the radiation incident on it. Calculations also showed that in the case of amplifying a dephased input signal (with a random phase shift of the input signal in each channel), this dephasing is also preserved in the output beam. Thus, it follows from the calculations that there are no fundamental obstacles to the efficient summation of radiation in a multichannel EPPL with an SBS mirror.

Figure 11 shows the near-field pattern of MO radiation amplified after the first pass before arriving at the SBS mirror, as well as the pattern of the Stokes radiation emerging from the SBS mirror before the second amplification pass. At the input of the amplifying channels, approximately the same intensity (~4 W cm^{-2}) reference radiation was formed. From Fig. 11a it can be seen that the amplification channels operation is approximately the same. The amplified MO radiation, i.e., the pump radiation for SBS, after angular selection, is directed into the cell with a nonlinear medium for SBS and phase conjugation. According to Fig. 11b, the Stokes radiation reflected from the SBS mirror in the near zone also consists of two beams separated by the required spatial interval, which quite impressively reflects the meaning of phase conjugation. The quality of the phase conjugation is very high, in full agreement with the calculations, and Fig. 11b also clearly shows the weakly expressed annular structure of the beam in each channel, which was demonstrated in the calculations [14–16].

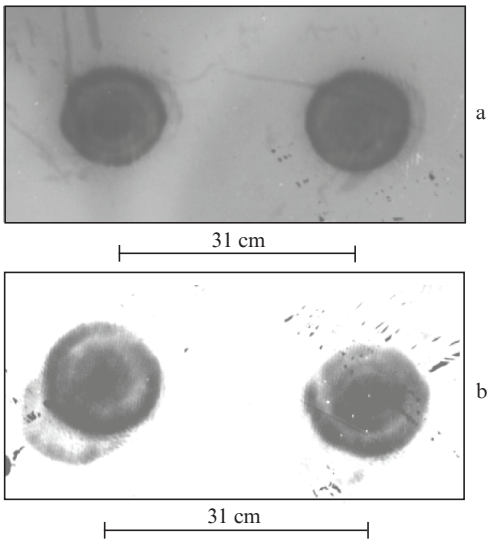

Figure 11. Experimental distribution of the energy density of (a) pump and (b) Stokes radiation in the near field.

The EPPL output radiation pattern in the near-field zone is shown in Fig. 12. It is in good agreement with the results in Fig. 10.

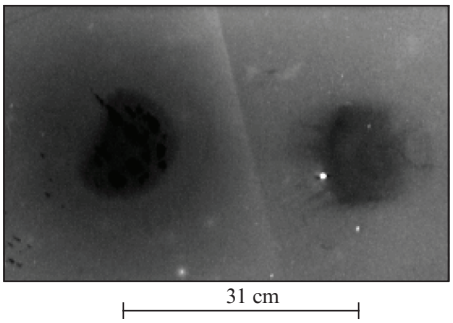

Figure 12. Energy density distribution of EPPL output radiation in the near-field zone.

Figure 13 allows a comparison of the calculated and experimental distributions of the EPPL radiation energy density in the plane of the MO aperture plotted on the same scale. The amplified Stokes radiation of two EPPL channels in the aperture plane at a distance of 2.5 km from the amplifier unit is an interference pattern of the radiation of two channels, and has a characteristic size of 8 cm and interference fringes with a characteristic size of about 1 cm. The total distribution width, which is determined by the radiation pattern from one channel, and the period of the interference fringes in the experiment and calculation are in good agreement. The circle indicates the MO aperture. The distance between the fringes of the pattern $\Delta x = \lambda L_1/\delta$, determined by the angle of convergence of the beams from the two channels, at $L_1 = 2.5$ km and $\delta = 31$ cm amounts to 1.0 cm, which is close to the data obtained in experiment and calculation. The lower contrast of the fringes in the experiment compared to the calculation is explained by the fact that the average input intensity is 4 W cm^{-2}, which is insufficient to suppress completely the effect of parasitic reflections of laser radiation from the elements of the optical scheme and self-excitation.

The maximum brightness of the EPPL radiation is observed near the optical axis, in the centre of the aperture, i.e., the central fringe of the pattern passes through it. The general slope of the wave front of each of the beams is also preserved under turbulence conditions. Several calculations have been performed with various implementations of a turbulent atmosphere in the case of a channelled phase conjugation combiner. The central fringe of the pattern passes through the centre of the aperture in all cases.

It is interesting to consider the operation of a two-channel EPPL, when the SBS mirror is replaced with a conventional reflective (100%) spherical mirror with a radius of curvature equal to the distance from the mirror to the MO aperture. Figure 14 shows the distribution pattern of the EPPL radiation energy density in the aperture plane obtained under conditions of a moderately turbulent atmosphere with $C_n^2 =$

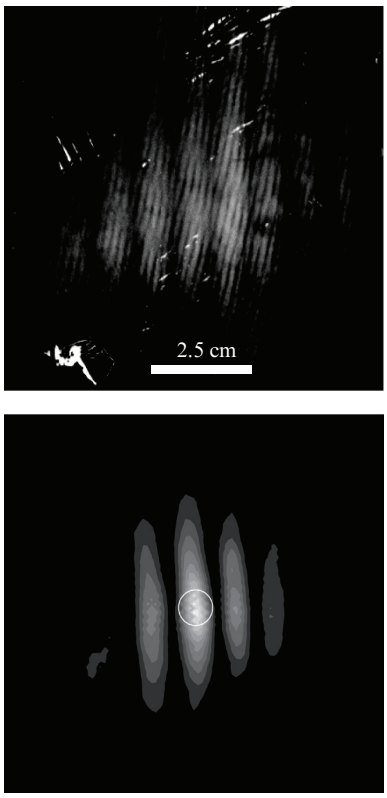

Figure 13. Distribution of the energy density of EPPL radiation in the plane of the MO aperture (a) in experiment and (b) calculation at $C_n^2 = 10^{-15}$ cm$^{-2/3}$.

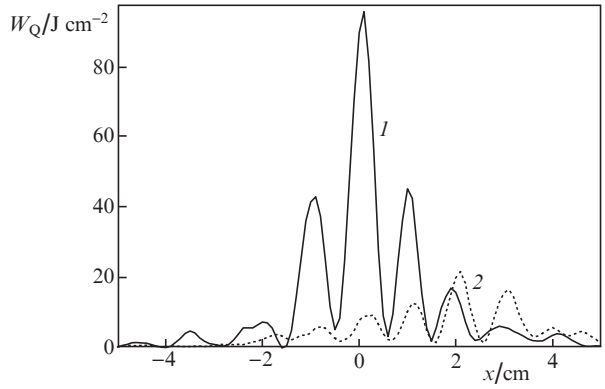

Figure 14. Section of the calculated radiation energy density distribution in the aperture plane in the case of a two-channel EPPL with (*1*) an SBS mirror and (*2*) a spherical mirror.

10^{-15} cm$^{-2/3}$ using a spherical mirror. In this case, the distribution of the energy density can be seen to be significantly broadened and shifted away from the aperture. As the calculation showed, the maximum value of the energy density decreases by more than 4 times. The results presented demonstrate the clear advantage of using the phase conjugation effect in SBS for efficient phase combining of radiations from many EPPL channels.

5. Conclusions

An experimental and computational and theoretical study of the operation of a two-channel EPPL in a 'converging version' with an SBS-mirror under conditions of a turbulent atmospheric path was performed. The distance between the axes of the channels was 31 cm. The radiation source in the form of an aperture 0.6 cm in diameter, from which the radiation of the explosively pumped MO emerges, is located at a distance of 2.5 km from the entrance to the amplifier unit.

It is found that the experimental distribution of the energy density of the output radiation in the plane of the aperture is an interference pattern of the radiation of two channels. The fringe width in the pattern is determined by the distance between the channels. The calculated energy density distribution in the aperture plane, obtained under conditions of moderate atmospheric turbulence ($C_n^2 = 10^{-15}$ cm$^{-2/3}$), agrees well with the experimental pattern in terms of the total distribution width and fringe width. According to the calculations, the maximum energy density in the aperture plane increases by more than 4 times compared to the case of a single-channel EPPL, both in a homogeneous and moderately turbulent atmosphere. The central fringe of the interference pattern passes through the centre of the aperture, i.e., the maximum energy density of the EPPL radiation is observed near the optical axis, in the centre of the aperture.

References

1. Basov N.G., Zuev V.S., Kirillov G.A. et al. *Preprint FIAN, No. 40* (Moscow, 1992).
2. Arzhanov V.P., Borovich B.P., Zuev V.S., et al. *Quantum Electron*., **22**, 118 (1992) [*Kvantovaya Elektron*., **19**, 135 (1992)].
3. Zeldovich B.Ya., Popovichev V.I., Ragulsky V.V., et al. *JETP Lett.*, **15**, 109 (1972) [*Pis'ma Zh. Eksp. Teor. Fiz*., **16**, 160 (1972)].
4. Nosach O.Yu., Popovichev V.I., Ragulsky V.V., Faizullov F.S. *JETP Lett*., **16**, 435 (1972) [*Pis'ma Zh. Eksp. Teor. Fiz*., **16**, 617 (1972)].
5. Dolgopolov Yu.V., Komarevsky V.A., Kormer S.B., et al. *J. Exp. Teor. Phys*., **49**, 458 (1979) [*Zh. Eksp. Teor. Fiz*., **76**, 908 (1979)].
6. Kulikov S.M., Dudov A.M., Dolgopolov Yu.V., et al. *Proc. SPIE*, **1628**, 90 (1992).
7. Kulikov S.M., Dolgopolov Yu.V., Dudov A.M., et al. *Laser Part. Beams*, **17**, 4 (1999).
8. Bobrov S.T., Gratsianov K.V., Kornev A.F., et al. *Opt. Spektrosk*., **62**, 402 (1987).
9. Kochemasov G.G., Starikov F.A. *Opt. Commun*., **170**, 161 (1999).
10. Starikov F.A., Dolgopolov Yu.V., Kochemasov G.G., et al. *Proc. SPIE*, **3930**, 12 (2000).
11. Starikov F.A., Dolgopolov Yu.V., Kovaldov S.A., et al. *Proc. SPIE*, **4184**, 445 (2001).
12. Starikov F.A., Dolgopolov Yu.V., Kovaldov S.A., et al. *Proc. SPIE*, **4353**, 202 (2001).
13. Starikov F.A., Dolgopolov Yu.V., Kovaldov S.A., et al. *Izv. Ross. Akad. Nauk, Ser. Fiz*., **65**, 935 (2001).
14. Starikov F.A., Dolgopolov Yu.V., Dudov A.M., et al. *Proc. SPIE*, **5137**, 165 (2003).
15. Starikov F.A., Dolgopolov Yu.V., Dudov A.M., et al. *Proc. SPIE*, **5147**, 60 (2003).
16. Starikov F.A., Dolgopolov Yu.V., Dudov A.M., et al. *Proc. SPIE*, **5479**, 81 (2004).
17. Starikov F.A., Dolgopolov Yu.V., Dudov A.M., et al. *Proc. SPIE*, **5777**, 307 (2005).
18. Rockwell D.A. *IEEE J. Quantum Electron*., **24**, 1124 (1988).
19. Andreev N.F., Babin A.A., Khazanov E.A., Paperny S.B., Pasmanik G.A. *Laser Phys*., **2**, 1 (1992).
20. Brignon A. (Ed.) *Coherent Laser Beam Combining* (Wiley-VCH, 2013) pp 427 – 478. DOI: 10.1002/9783527652778.
21. Kong H.J., Lee S.K., Lee D.W. *Laser Part. Beams*, **23**, 5559 (2005).
22. Bogachev V.A., Garanin S.G., Dolgopolov Yu.V. *Quantum Electron*., **42**, 531 (2012) [*Kvantovaya Elektron*., **42**, 531 (2012)].
23. Volkov V.A., Volkov M.V., Garanin S.G., Starikov F.A. *Quantum Electron*., **45**, 1125 (2015) [*Kvantovaya Elektron*., **45**, 1125 (2015).